Development of an artificial vision system that allows non-destructive testing on flat concrete slabs for surface crack detection by processing of digital images in MATLAB.

BE-Romero-Tarazona[1], CL-Rodriguez-Sandoval[1], JG-Villabona1-Ascanio[1], A D Rincón-Quintero[1,2].

[1] Automation and Control Energy Systems Research Group (GISEAC), Design and materials research group (DIMAT), Electromechanical Engineering, Faculty of Natural Sciences and Engineering, Technological Units of Santander (UTS), Road No 9-82 students, 680,005, Bucaramanga, Colombia.
[2] Energy in Building research group (ENEDI), Doctoral Program in Energy Efficiency and Sustainability in Engineering and Architecture, Department of Machines and Thermal Engines, University of the Basque Country (UPV/EHU), Engineer Torres Quevedo Plaza, 1, 48013, Bilbao, BI, España

btarazona@correo.uts.edu.co

Abstract. A computing tool based on an intelligent algorithm generates new alternatives for an early crack detection on flat concrete slab in a surface testing. First, a system able to autonomously detect a surface crack, by means of a digital image processing system has been developed. This system carries on an effective selection of data by an algorism bound to a specialized MATLAB software that can assess in full detail the surface conditions of a concrete slab, and finding out any affected spot.

1. Introduction

Cracks are breaking sites occurring in concrete when the tensions stressing the concrete structures are superior to its resistance. Several conditions leading to this serious threat, some or chemical origin, other of physical origin. Depending on the time they first appear, it could be in the fresh stage or plastic stage, before the hardening has taken place, or in other instances, through the concrete hardening process [1].

It is here when the term durability arises. Durability may be defined as the concrete structure capacity to keep intact both their chemical and physical attributes throughout their usable life span when subjected to material break up as a result of multiple tensions these structures are designed to resist. Therefore, every potentially aggressive agent a concrete structure is exposed to, must be identified [2].

In turn, the first indications of structural degradation in particular are given in superfie thereof, evidenced as fissures and cracks [3], Locally reducing the stiffness and causing discontinuities in the material[4] [5], Which affects the durability of the structure and is critical for maintenance, because they remain in contact with the environment causing severe damage [3]. Several authors mention in their research technique crack detection by manual visual inspection, one says that it is the method most

commonly used in practice, which is inefficient from the standpoint of cost, time, accuracy and safety[6]Another describes it as; the method acclaimed for inspecting cracks, stresses that the manual inspection, the outline of the crack or fissure is prepared manually and conditions of irregular observed, depending entirely on the knowledge and experience of the specialist, lacking a quantitative analysis[3].

But basically crack detection can be done in two ways, using destructive or non-destructive testing, for example, through the inclusion of visual tools and topographic examination assessing the deficiencies of surface [7] as a nondestructive method, as well as automatic detection, which is very effective [8], Which uses some techniques such as infrared and thermal test[9] [10], Ultrasonic testing[eleven], Laser test[12]and radiographic test[13]. Added to this, many detection methods through image processing[14]They have been highly proposed by automation, objectivity and efficiency. However, there are many difficulties in detection for various reasons[fifteen]. Methods based on image processing are summarized and divided into four categories[3] [15] : Integrated algorithm [16], Morphological approach[17]Method based on percolation[18], Technical practice, among others.

A promising alternative methods are based on computer vision that can automatically extract information from the cracks of images. Binarization image, developed for detecting text is appropriate for identifying cracks, since the texts and cracks are similar and consist of lines and curves distinguishable. However, standardizing identifying cracks using binarization image is a challenge because the binarization depends on the method and associated parameters[19].

Thus, it has experienced a growing interest in developing tools to analyze images (flat slabs) by nondestructive testing and Technological Units of Santander have a Laboratory of Industrial Control and Automation, which lacked a specialized software capable determining the existence of cracks on flat slabs, why this document presents the development of an algorithm capable of detecting independently the crack, by digital image processing using MATLAB. The purpose of the system is to allow detailed assessment of structures to analyze, locating the areas affected by the above-mentioned phenomenon.

2. Materials and Methods

2.1. materials

2.1.1. Camera. The camera used to capture the images before starting the process of analysis, brand Nikon D5300 camera is Wi-Fi + 18-55 mm lens, 24 megapixel.

2.1.2. MATLAB. To develop the algorithm will use the software MATLAB, which is a computing environment that enables the execution of numerical and symbolic calculations quickly and accurately, accompanied by graphic features and advanced visualizations Aptar for scientific work in engineering[20].

2.1.3. Computer. the use of a computer capable of running the MATLAB software for algorithm development and subsequent commissioning is required.

2.1.4. flat concrete slabs. It is required for the project, study material concrete, in Figure 1 the flat plates 6 Concrete used in the project proposed herein which were made and used in a previous project are evidenced by[21]With the following characteristics:

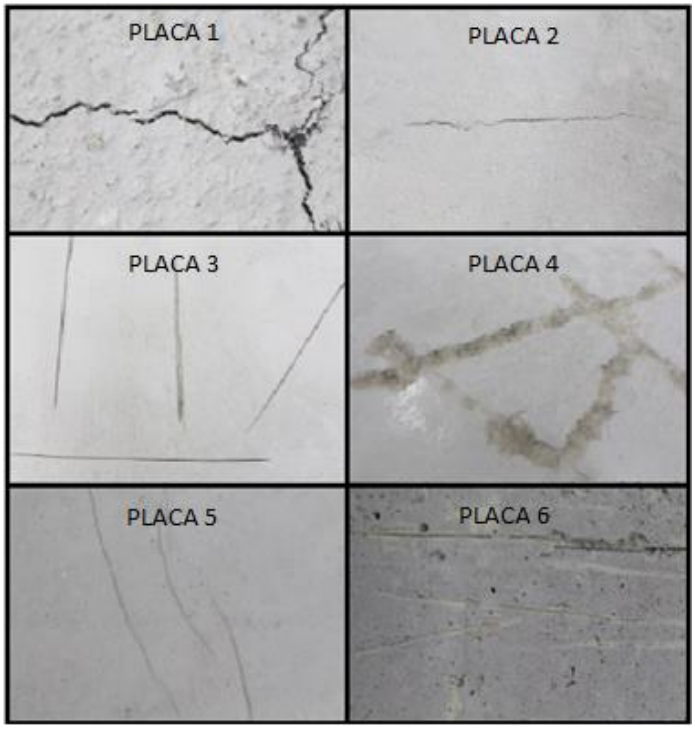

Figure 1. Flat plates Concrete

Mixture of sand, crushed, cement and water (3000 PSI Concrete), weight 65 kg.
Plate 1: Reflects minor cracks in the center. (Natural fissure)
PLATE 2: Reflects a small crack on the right side. (Natural fissure)
PLATE 3: 4 large cracks that reflects through the plate vertically and horizontally. (Created with a polisher)
Plate 4: Reflects fissure caused by chisel, with enamel finish.
PLATE 5: Reflects minor cracks. PLATE 6: Reflected multiple cracks, fissures and discontinuities mild throughout its structure. (Natural fissure)

2.2. Method

The methodology for the development of artificial vision system seeks to develop a tool capable of performing digital image processing in order to enhance images taken initially to flat concrete slabs and create a new one, in which the surface discontinuities is evident . The initial process requires a photographic record of the plates made with a NIKON D5300 described above, was considered lighting surrounding the plate in order to capture the image with adequate contrast, the process of making or photographic survey was conducted by a professional photographer. Subsequently, the algorithm can process images is developed for this, The experimental design is performed to determine how to treat the image properly with the digital image processing, in order to obtain an inspection or non-destructive testing of such structures hormigo with surface problems fissures type further determining area affectation. Figure 2 evidence the steps required for methodological development project.

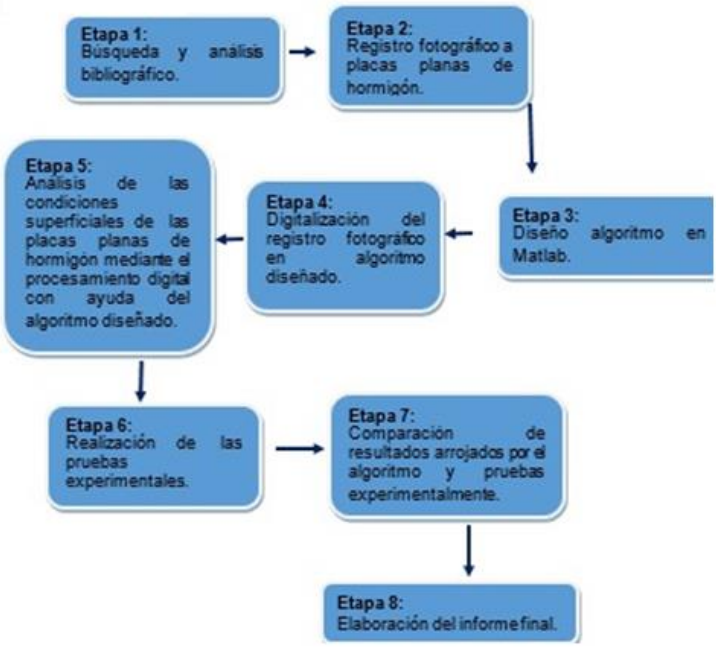

Figure 2 Flow diagram

3. Tests and results

a photographic record for digital processing and analysis of the images later, which is closely linked to the quality of the image capture rose. NIKON D5300 camera and technical services of a professional photographer was used for making initial images. In Figure 3, an unspecified images taken in the process prior to capture the same processing algorithm developed percentage is reflected.

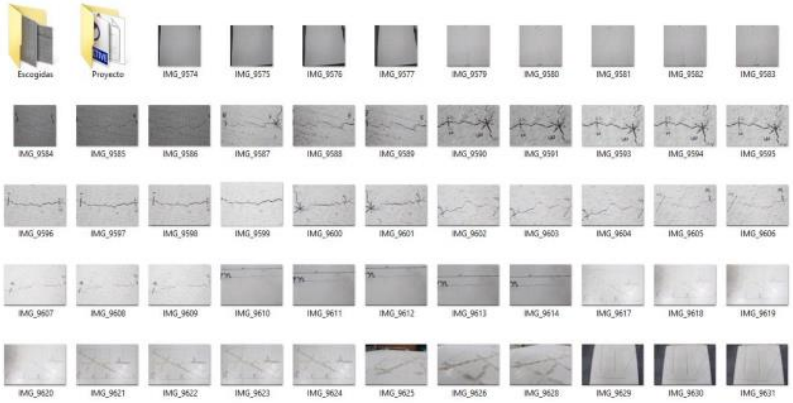

Figure 3 Photographic record

They took a total of 130 photos, taking into account three aspects to select appropriate: Sharpness, position (location and focus) and quality.

Subsequently, the algorithm is designed in MATLAB, is which performs an initial process of image recognition to pass to grayscale, apply a spatial filter, then converted to a binary image with a threshold and morphologic arrangements (Apertura and closing), preceded by process histogram, to finally have the binarized image arranged and the calculation of the impact area, figure 4 shows the methodological above mentioned process performed by the algorithm designed.

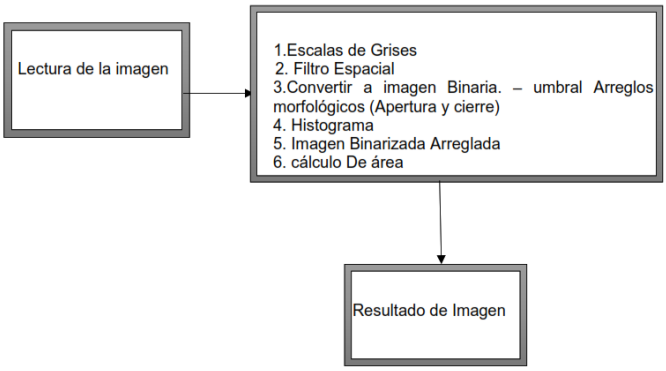

Figure 4 Flowchart image processing

Development work was important the realization of an experimental design in order to obtain information with the smallest number of experiments, based on the central objective was to measure how they influence K factors in identifying discontinuities in images by digital image processing in MATLAB.

For simplicity, an array of full factorial experiments provides the least number of tests which can be studied k factors in a full factorial design2^k[22].

Factorial design with the effect of two factors considered two levels in each study. Each replica of this design is 2x2 combinations or treatments that may denote different ways, reflected in Table 1.2^2

Table 1. How to write the treatment design

Factor A	Factor B	Reply y
-	-	$y_{11}(o)$
+	-	$y_{21}(a)$
-	+	$y_{12}(b)$
+	+	$y_{22}(ab)$

X = Alteration of structure-> "Independent".

Y = Process image for the alteración-> (filtering, morphological arrangements). "Dependent"

This design is the simplest of the series, considering two factors f1 and f2, each two levels. It can be represented geometrically as a square with 4 trials.

F1 = morphologic Arrangement (opening and closing) = (square "square" Create a square structuring element whose width is w pixels, w should be a non-negative integer, disk "disk" Create a flat structuring element disk-shaped, where R specifies the radius. R must be a nonnegative integer.

F2 = spatial filter = (average "Average" Returns an averaging filter argument can be a vector that specifies the number of rows and columns in which case it is a square matrix, disk "Averaged circulate" Returns an averaging filter within circular the square matrix side) creates a predetermined two-dimensional filter

Algebraic signs to calculate design effects 2^2.

Tests were from four trials per plate for a total of 4x6 = 24 TESTS. Each test was performed with different MATLAB programming with different variations of filter, but with the same image processing on the four tests.

one. Y11 = 1 = PROTOTYPE TEST (Disk, square)

two. Y21 = PROTOTYPE TEST 2 = (Disk, disk)

3. Y12 = PROTOTYPE TEST 3 = (Average, square)

4. Y22 = PROTOTYPE TEST 4 = (Average, disk)

Table 2. Matrix factorial design experiments for 2 ^ 2

Combination treatments	Spatial filter (Average)	Spatial filter (Disk)	Spatial filter (Average)	Spatial filter (Disk)
Morphological Arrangements (Square)	1	0	0	0
Morphological Arrangements (Square)	0	1	0	0
Morphological Arrangements (Disk)	0	0	1	0
Morphological Arrangements (Disk)	0	0	0	1

4 programming prototypes were made in MATLAB, the result of experimental design to determine which facilitate the identification of the Fissure additionally calculating the area of the same in the study material. They were taken into account morphological and spatial filtering arrangements in experimental design.

Algorithm developed the prototype 1 is shown below:

```
close all
clear all
clc

%% Read  the image
[a b] = uigetfile({'*.jpg','All Files'});
I= imread([b a]);
%I = imread('fotos\Placa 1-7.jpg');
%% Convert the image to grayscale
Igray = rgb2gray(I);
%% Average spatial filter
H = fspecial('disk',5);
Ifilter1=imfilter(Igray,H);
imshow(Ifilter1)
%% Convert to binary image
imgBW=im2bw(Ifilter1,0.65); % Convert the image to a binary  image
using the threshold
se= strel('square',3);
I3 = imopen(imgBW,se);
I3 = imclose(I3,se);
I3=~I3;
I4= bwareaopen(I3,5000);
[L Ne]=bwlabel(I4);
RGB = label2rgb(L,'jet','k');

% Figures
figure(1),imshow(I),title('Original image');
figure(2),imshow(Igray),title('Grayscale image');
figure(3),imshow(Ifilter1),title('Filteres image');
```

```
30 - figure(4),imhist(Ifilter1),title('Histogram');
31 - figure(5),imshow(I3),title('Binarized Image');
32 - figure(6),imshow(I4),title('Fixed Binarized Image');
33 - figure(7),imshow(RGB),hold on;
34 -
35 - prop = regionprops(L,'Centroid','Area');
36 - areas=[prop.Area]';
37 -
38 - for cnt=1:length(prop)
39 - text(prop(cnt).Centroid(1),prop(cnt).Centroid(2),num2str(label(cnt)),'Fon
40 - tSize',15,'color','white');
41 - end
```

4 prototypes were made, each prototype performs tests on the 6 plates to determine which of the four allows to prove the existence of fissures in the plates, determining in turn the area of affectation of the plates. Figure 5 shows the result of one of the images initially taken from the Concrete 01 plate and the image after the revision by the artificial vision system with a numbering by zones evaluated by the algorithm in the image processing.

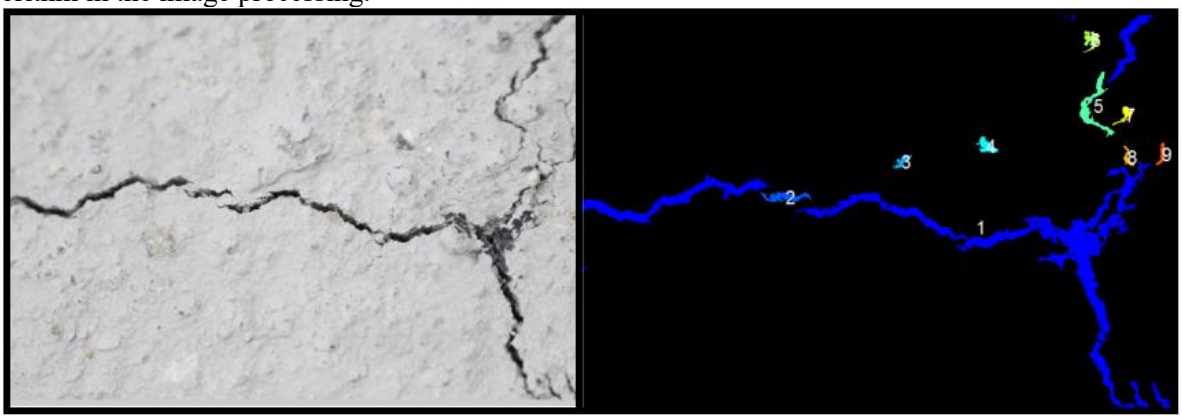

Figure 5 Treatment plate 1 prototype Algorithm 1

Table 3 reflects in column 2 the values of the pixel area corresponding to each of the zones evaluated by the algorithm, Figure 5 shows in the image processed by the algorithm the section corresponding to each number in the first column of the table, further in column three is the value of the centroid of the area pixelated by the vision system. with a numbering by zones evaluated by the algorithm in the image processing.

Table 3. Data plate processing 1 algorithm 1

Fields	Área	Centroid
1	741612	[3.4516e+03…
2	21701	[1.7783e+03…
3	7142	[2.7981e+03…
4	12954	[3.5437e+03…
5	36187	[4.4869e+03…
6	13451	[4.4601e+03…
7	8558	[4.7612e+03…
8	5377	[4.7791e+03…
9	6330	[5.0810e+03…

Figure 6 shows the result of one of the images taken from the Concrete plate 2 and the image after the revision by the artificial vision system with a numbering by zones evaluated by the algorithm in the processing of the image.

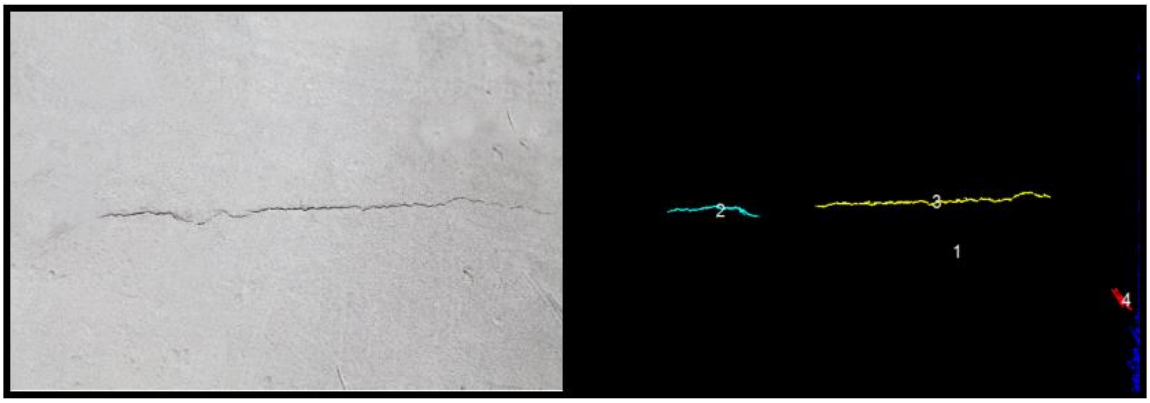

Figure 6 Treatment 2 plate prototype Algorithm 1

Table 4 reflects in column 2 the values of the pixel area corresponding to each of the zones evaluated by algorithm 1 on plate 2, Figure 6 shows in the image processed by the algorithm the section corresponding to each number in the first column of the table, additionally in column three is the centroid value of the pixelated area by the vision system.

Table 4. Data plate processing 2 algorithm 1

Fields	Área	Centroid
1	82116	[3.4959e+03…
2	15587	[1.3534e+03…
3	38118	[3.3073e+03…
4	9796	[5.0166e+03…

Figure 7 reflects the result of one of the images taken from the Concrete plate 3 and the image after the revision by the artificial vision system with a numbering by zones evaluated by the algorithm in the processing of the image.

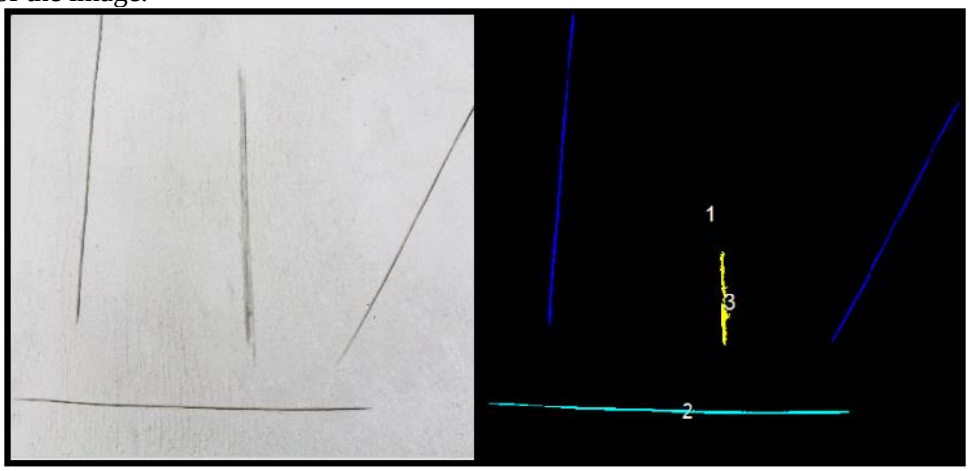

Figure 7 Treatment plate 3 prototype Algorithm 1

Table 5 reflects in column 2 the values of the pixel area corresponding to each of the zones evaluated by algorithm 1 on plate 3, Figure 7 shows in the image processed by the algorithm the section corresponding to each number in the first column of the table, additionally in column three is the centroid value of the pixelated area by the vision system.

Table 5. Data plate processing 3 algorithm 1

Fields	Área	Centroid
1	98767	[1.6544e+03…

2	47515	[1.4882e+03…
3	18035	[1.7870e+03…

Figure 8 reflects the result of one of the images taken from the Concrete plate 4 and the image after the revision by the artificial vision system with a numbering by zones evaluated by the algorithm in the processing of the image.

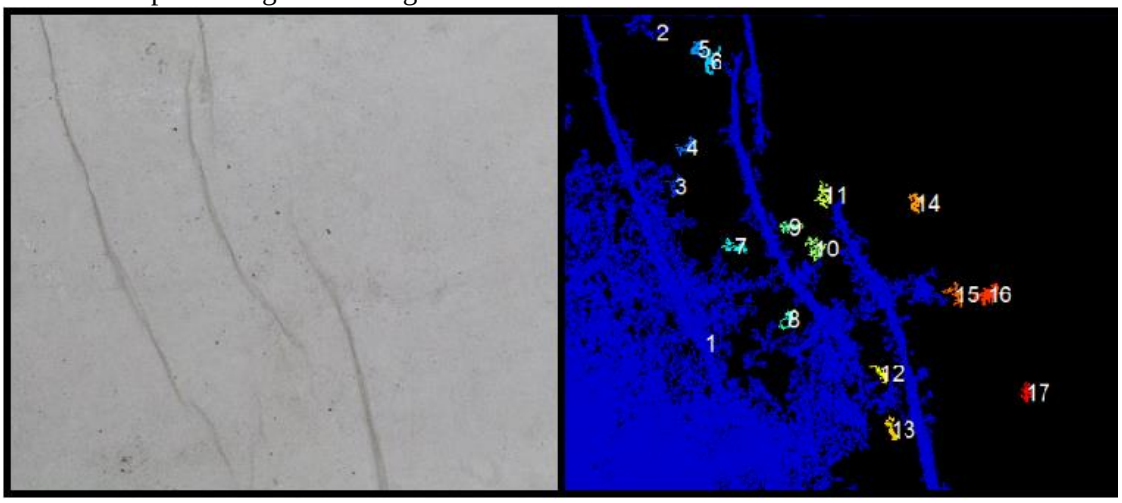

Figure 8 Treatment 4 plate prototype Algorithm 1

Table 6 reflects in column 2 the values of the pixel area corresponding to each of the zones evaluated by algorithm 1 on plate 4, Figure 8 shows in the image processed by the algorithm the section corresponding to each number in the first column of the table, additionally in column three is the centroid value of the pixelated area by the vision system.

Table 6. Data plate processing 4 algorithm 1

Fields	Área	Centroid
1	383602	[1.0626e+03…
2	5783	[721.1587 1…
3	6877	[855.7598 1…
4	6827	[938.4011 9…
5	5749	[1.0154e+03…
6	9068	[1.1087e+03…
7	6702	[1.2788e+03…
8	5910	[1.6573e+03…
9	5754	[1.6682e+03…
10	11106	[1.8514e+03…
11	8062	[1.9130e+03…
12	5342	[2.3167e+03…
13	6376	[2.3941e+03…
14	6738	[2.5701e+03…
15	8399	[2.8473e+03…
16	14721	[3.0804e+03…
17	5363	[3.3512e+03…

Figure 9 reflects the result of one of the images taken from the Concrete plate 05 and the image after the revision by the artificial vision system with a numbering by zones evaluated by the algorithm in the processing of the image.

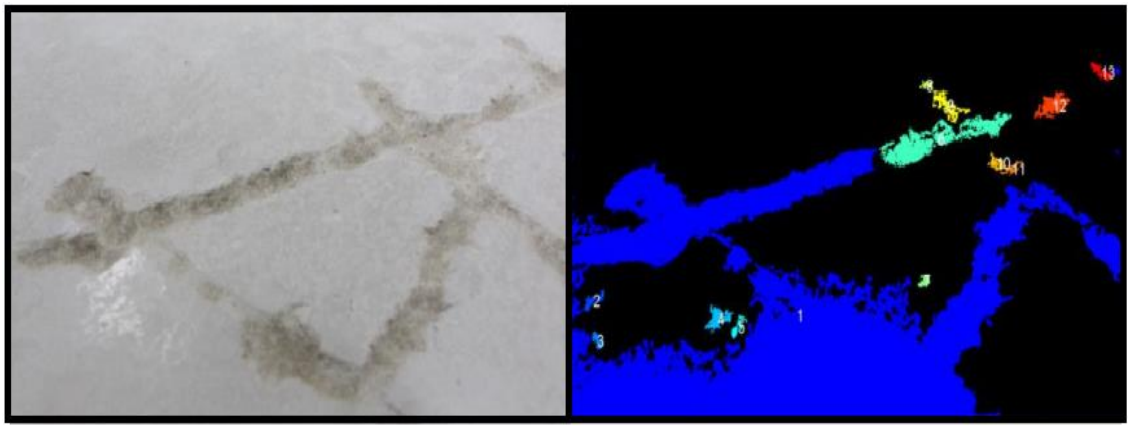

Figure 9 Treatment plate 5 prototype Algorithm 1

Table 7 reflects in column 2 the values of the pixel area corresponding to each of the zones evaluated by algorithm 1 on plate 5, in Figure 9, the image processed by the algorithm shows the section to which each number in the first column of the table corresponds, additionally in column three is the centroid value of the pixelated area by the vision system.

Table 7. Data plate processing 5 algorithm 1

Fields	Área	Centroid
1	4120220	[2.1330e+03…
2	10421	[217.5636 2…
3	6788	[257.3088 2…
4	21715	[1.3890e+03…
5	7849	[1.5792e+03…
6	150884	[3.4610e+03…
7	5979	[3.3304e+03…
8	5045	[3.3526e+03…
9	25299	[3.3525e+03…
10	9482	[4.0132e+03…
11	6174	[4.1553e+03…
12	32352	[4.5378e+03…
13	11408	[4.9983e+03…

Figure 10 reflects the result of one of the captured images of the concrete slab 06, the post review by the artificial vision system evaluated by the algorithm 01 image and no data values corresponding to specific areas.

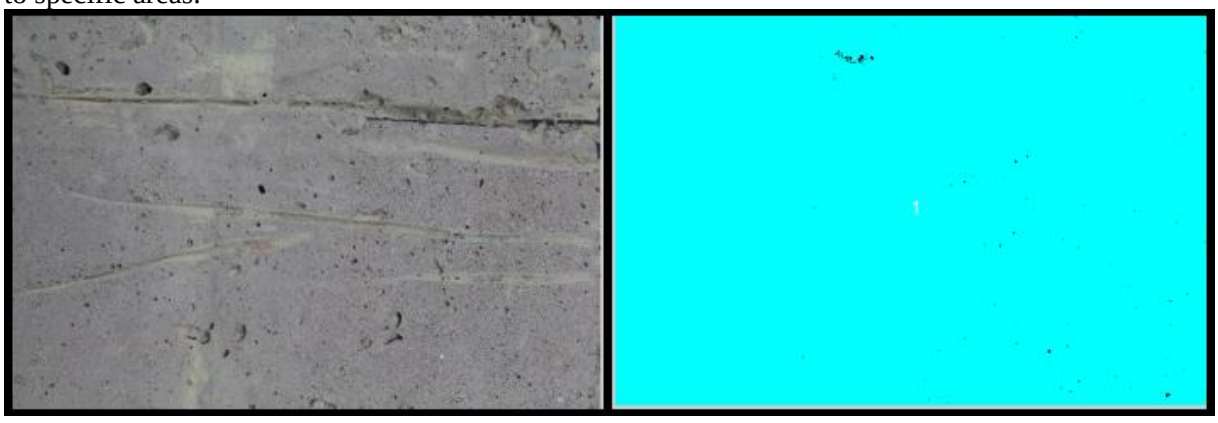

Figure 10 Treatment plate 6 prototype Algorithm 1

Next, the results of the other three algorithms performed in the process of executing the design of experiments, the algorithms are not included, only the images corresponding to those previously presented by algorithm 01, to facilitate the analysis of the results in this document. Figure 11 shows the result of one of the images initially taken from the Concrete plate 01 and the image after the revision by the artificial vision system with a numbering by zones evaluated by the algorithm in the image processing.

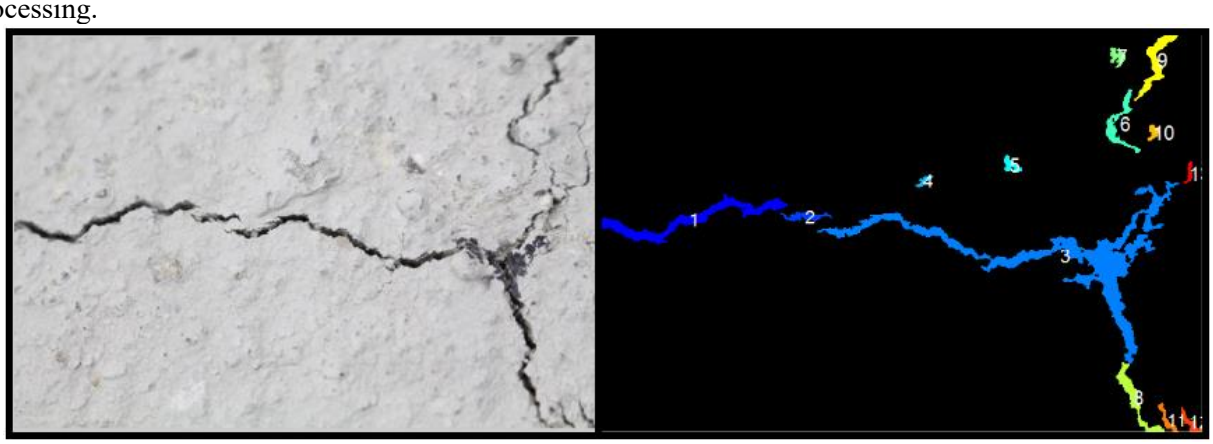

Figure 11 Treatment 1 prototype board Algoritmo2

Table 8 reflects in column 2 the values of the pixel area corresponding to each of the zones evaluated by algorithm 2 on plate 1, Figure 11 shows in the image processed by the algorithm the section corresponding to each number in the first column of the table, additionally in column three is the centroid value of the pixelated area by the vision system.

Table 8. Data plate processing 1 algorithm 2

Fields	Área	Centroid
1	129400	[782.9074 1…
2	21597	[1.7774e+03…
3	444908	[3.9764e+03…
4	7214	[2.7982e+03…
5	12809	[3.5443e+03…
6	358334	[4.4854e+03…
7	13211	[4.4613e+03…
8	44307	[4.6042e+03…
9	51704	[4.8009e+03…
10	8030	[4.7720e+03…
11	11215	[4.8830e+03…
12	12105	[5.0802e+03…
13	6195	[5.0821e+03…

Figure 12 reflects the result of one of the images initially captured from the Concrete plate 2 and the image after the revision by the artificial vision system with a numbering by zones evaluated by the algorithm in the image processing.

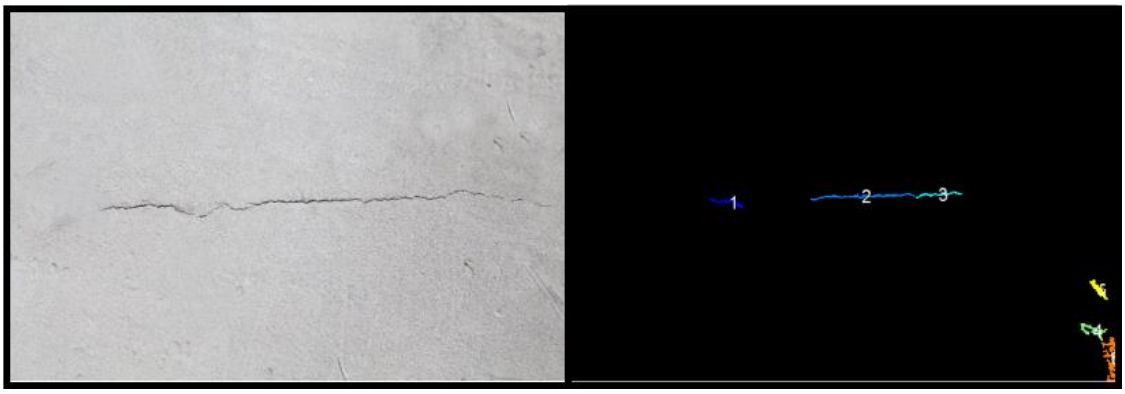

Figure 12 Treatment 2 prototype board Algoritmo2

Table 9 reflects in column 2 the values of the pixel area corresponding to each of the zones evaluated by algorithm 2 on plate 2, Figure 12 shows in the image processed by the algorithm the section corresponding to each number in the first column of the table, additionally in column three is the centroid value of the pixelated area by the vision system.

Table 9. Data plate processing 2 algorithm 2

Fields	Área	Centroid
1	7822	[1.5204e+03…
2	18128	[2.7843e+03…
3	8818	[3.5019e+03…
4	11453	[4.9627e+03…
5	10897	[5.0159e+03…
6	26020	[5.1376e+03…

Figure 13 reflects the result of one of the images initially captured from the Concrete plate 3 and the image after the revision by the artificial vision system with a numbering by zones evaluated by the algorithm in the image processing.

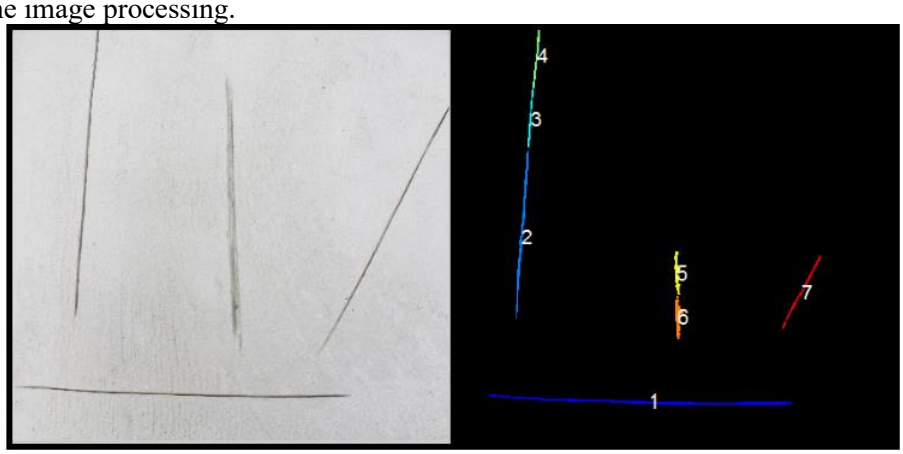

Figure 13 Treatment 3 prototype board Algoritmo2

Table 10 reflects in column 2 the values of the pixel area corresponding to each of the zones evaluated by algorithm 2 on plate 3, in Figure 13 the image processed by the algorithm shows the section corresponding to each number in the first column of the table, additionally in column three is the centroid value of the pixelated area by the vision system.

Table 10. Data plate processing 3 algorithm 2

Fields	Área	Centroid
1	44640	[1.5645e+03…

2	23627	[564.7436 1…
3	7037	[632.9156 7…
4	7793	[680.9493 2…
5	7607	[1.7826e+03…
6	10017	[1.7907e+03…
7	9977	[2.7607e+03…

Figure 14 reflects the result of one of the images initially captured from the Concrete plate 4 and the image after the revision by the artificial vision system with a numbering by zones evaluated by the algorithm in the image processing.

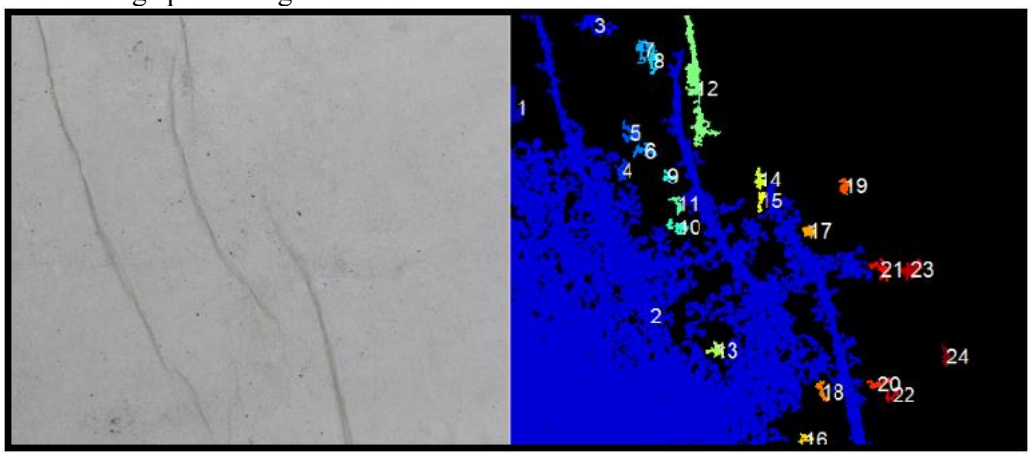

Figure 14 Treatment 4 prototype board Algoritmo2

Table 11 reflects in column 2 the values of the pixel area corresponding to each of the zones evaluated by algorithm 2 on plate 4, Figure 14 shows in the image processed by the algorithm the section corresponding to each number in the first column of the table, additionally in column three is the value of the centroid of the pixelated area by the vision system.

Table 11. Data plate processing 4 algorithm 2

Fields	Área	Centroid
1	18456	[42.1052 73…
2	4277608	[1.0742e+03…
3	24302	[652.8055 8…
4	9043	[857.6036 1…
5	1293	[922.6540 9…
6	9986	[1.0331e+03…
7	11151	[1.0242e+03…
8	8783	[1.0972e+03…
9	5134	[1.2110e+03…
10	10519	[1.2868e+03…
11	5678	[1.2815e+03…
12	72177	[1.4265e+03…
13	8276	[1.5806e+03…
14	9090	[1.9140e+03…
15	5760	[1.9199e+03…
16	6419	[2.2624e+03…
17	5936	[2.2952e+03…
18	7095	[2.3943e+03…
19	7868	[2.5711e+03…
20	8331	[2.8256e+03…
21	11176	[2.8455e+03…

22	5507	[2.9339e+03…
23	16717	[3.0797e+03…
24	7379	[3.3480e+03…

Figure 15 reflects the result of one of the images initially captured from the Concrete plate 5 and the image after the revision by the artificial vision system with a numbering by zones evaluated by the algorithm in the image processing.

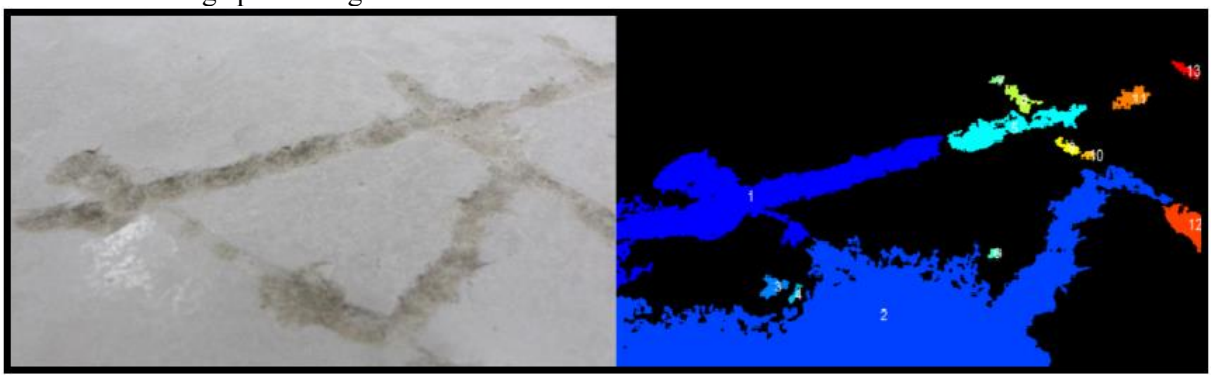

Figure 15 Plate treatment 5 prototype Algoritmo2

Table 12 reflects in column 2 the values of the pixel area corresponding to each of the zones evaluated by algorithm 2 on plate 5, Figure 15 shows in the image processed by the algorithm the section corresponding to each number in the first column of the table, additionally in column three is the value of the centroid of the pixelated area by the vision system.

Table 12. Data plate processing 5 algorithm 2

Fields	Área	Centroid
1	979627	[1.1568e+03…
2	3121096	[2.3252e+03…
3	24373	[1.3874e+03…
4	8102	[1.5758e+03…
5	165189	[3.4711e+03…
6	6453	[3.3298e+03…
7	5592	[3.3513e+03…
8	27349	[3.5586e+03…
9	15762	[3.9794e+03…
10	5610	[4.1573e+03…
11	35271	[4.5369e+03…
12	77571	[5.0315e+03…
13	14832	[5.0148e+03…

Figure 16 reflects the result of one of the captured images of the concrete plate 06, the post review by the artificial vision system evaluated by the algorithm 02 image and no data values corresponding to specific areas.

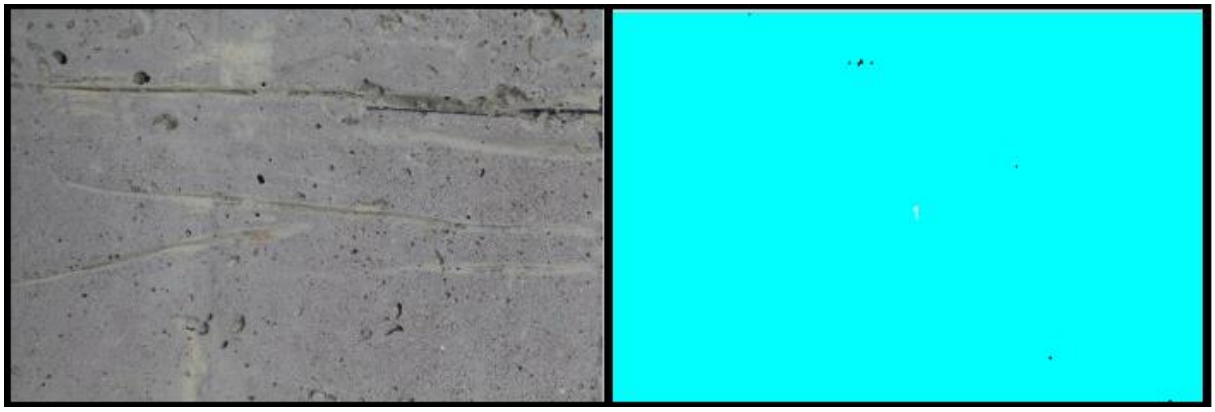

Figure 16 Treatment 6 prototype board Algoritmo2

Furthermore, the results of the image processing provided by Algorithm 03 begin in Figure 17, that evidences the result of one of the images initially captured from the Concrete plate 01 and the image after the revision by the system of artificial vision with a numbering by zones evaluated by the algorithm in the image processing.

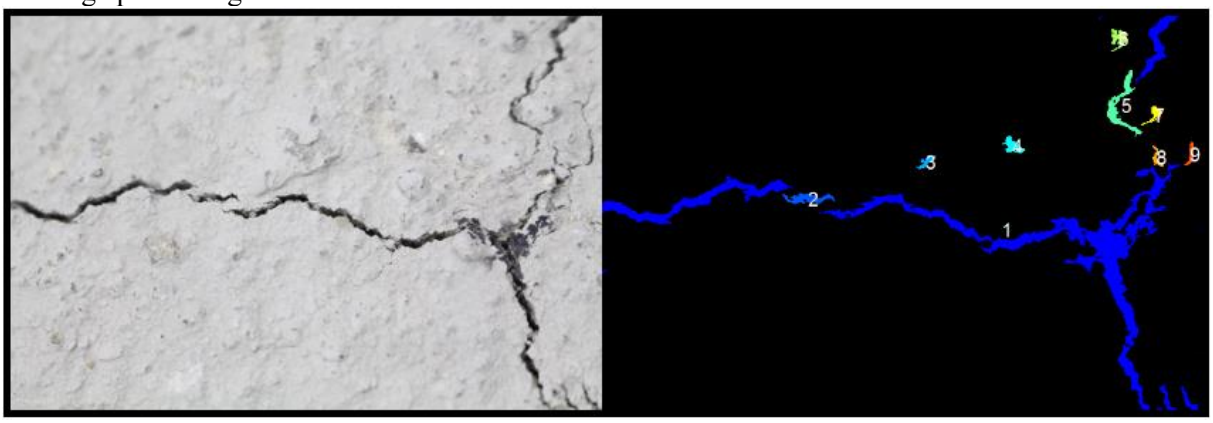

Figure 17 Treatment 1 plate prototype Algorithm 3

Table 13 reflects in column 2 the values of the pixel area corresponding to each of the zones evaluated by algorithm 3 on plate 1, Figure 17 shows in the image processed by the algorithm the section corresponding to each number in the first column of the table, additionally in column three is the value of the centroid of the pixelated area by the vision system

Table 13. Data plate processing 1 algorithm 3

Fields	Área	Centroid
1	753595	[3.4514e+03…
2	21824	[1.7777e+03…
3	7137	[2.7976e+03…
4	12959	[3.5432e+03…
5	36286	[4.4864e+03…
6	12461	[4.4598e+03…
7	8586	[4.7608e+03…
8	5421	[4.7787e+03…
9	6397	[5.0805e+03…

Figure 18 reflects the result of one of the images initially captured Concrete plate 02 and the image after the revision by the system of artificial vision with a numbering by zones evaluated by the algorithm in the image processing.

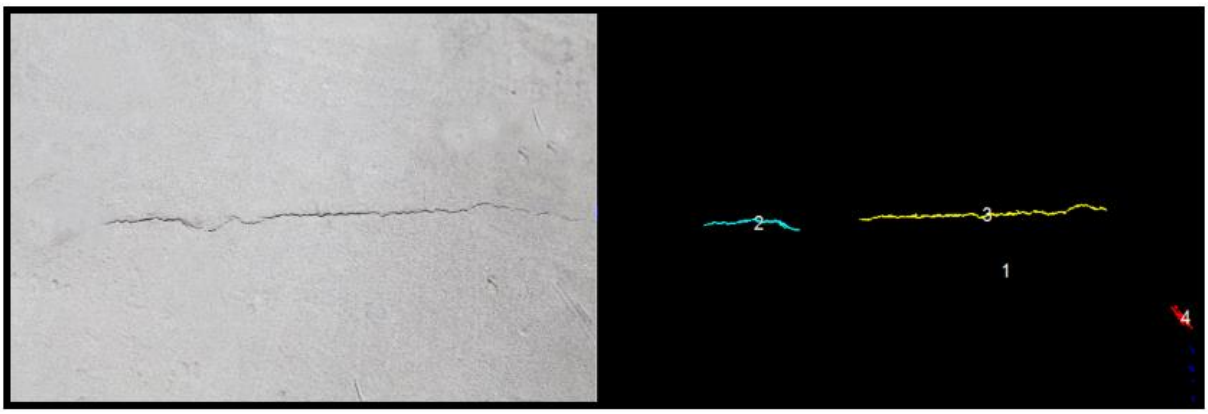

Figure 18 Treatment 2 plate prototype Algorithm 3

Table 14 reflects in column 2 the values of the pixel area corresponding to each of the zones evaluated by algorithm 3 on plate 2, Figure 18 shows in the image processed by the algorithm the section corresponding to each number in the first column of the table, additionally in column three is the value of the centroid of the pixelated area by the vision system

Table 14. Data plate processing 2 algorithm 3

Fields	Área	Centroid
1	88895	[3.4656e+03…
2	15973	[1.3523e+03…
3	39264	[3.3079e+03…
4	9795	[5.0160e+03…

Figure 19 reflects the result of one of the images initially captured Concrete plate 03 and the image after the revision by the system of artificial vision with a numbering by zones evaluated by the algorithm in the image processing.

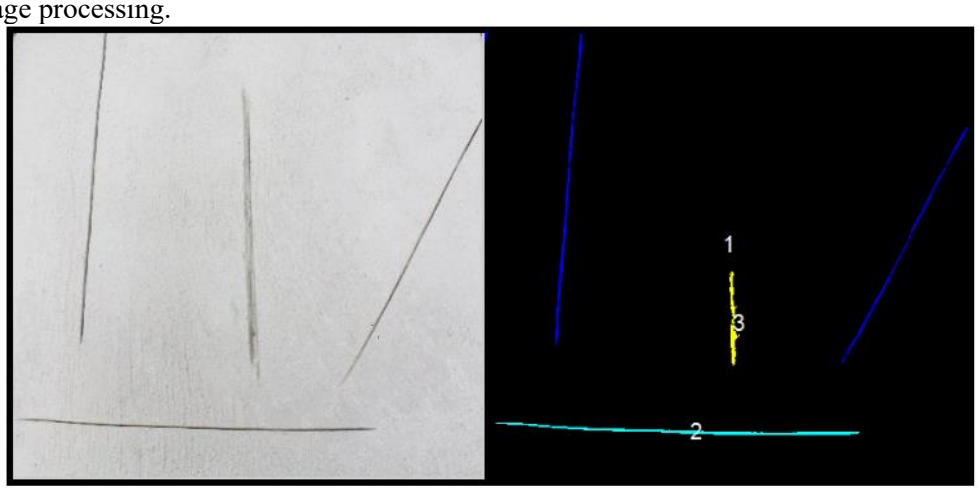

Figure 19 Treatment 3 prototype plate Algorithm 3

Table 15 reflects in column 2 the values of the pixel area corresponding to each of the zones evaluated by algorithm 3 on plate 3, Figure 19 shows in the image processed by the algorithm the section corresponding to each number in the first column of the table, additionally in column three is the value of the centroid of the pixelated area by the vision system

Table 15. Data plate processing 3 algorithm 3

Fields	Área	Centroid
1	105587	[1.7204e+03…

2	48706	[1.4867e+03…
3	18056	[1.7865e+03…

Figure 20 reflects the result of one of the images initially captured Concrete plate 04 and the image after the revision by the system of artificial vision with a numbering by zones evaluated by the algorithm in the image processing.

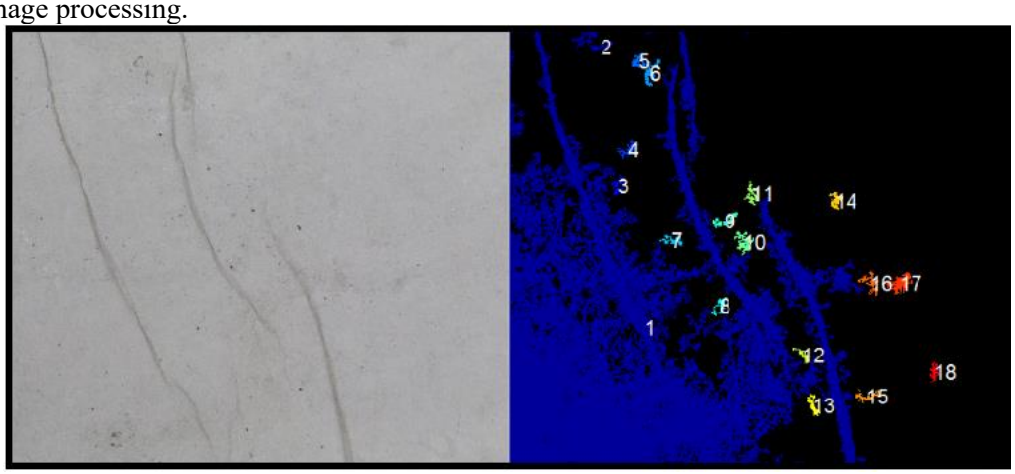

Figure 20 Treatment 4 plate prototype Algorithm 3

Table 16 reflects in column 2 the values of the pixel area corresponding to each of the zones evaluated by algorithm 3 on plate 4, Figure 20 shows in the image processed by the algorithm the section corresponding to each number in the first column of the table, additionally in column three is the value of the centroid of the pixelated area by the vision system

Table 16. Data plate processing 4 algorithm 3

Fields	Área	Centroid
1	763595	[3.5714e+03…
2	11824	[1.7877e+03…
3	7937	[2.9976e+03…
4	12959	[3.9432e+03…
5	37786	[4.4334e+03…
6	12871	[4.4128e+03…
7	8766	[4.7008e+03…
8	5991	[4.7007e+03…
9	6897	[5.9805e+03…

Figure 21 reflects the result of one of the images initially captured Concrete plate 05 and the image after the revision by the system of artificial vision with a numbering by zones evaluated by the algorithm in the image processing.

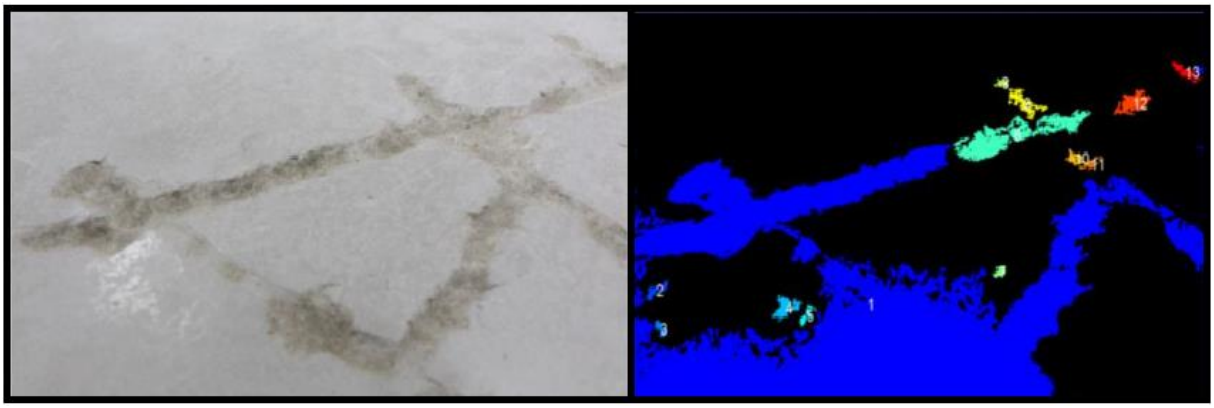

Figure 21 Treatment plate 5 prototype Algorithm 3

Table 17 reflects in column 2 the values of the pixel area corresponding to each of the zones evaluated by algorithm 3 on plate 5, Figure 21 shows in the image processed by the algorithm the section corresponding to each number in the first column of the table, additionally in column three is the value of the centroid of the pixelated area by the vision system

Table 17. Data plate processing 5 algorithm 3

Fields	Área	Centroid
1	4130228	[2.1341e+03…
2	10418	[217.1615 2…
3	6792	[256.6637 2…
4	21886	[1.3881e+03…
5	7890	[1.5785e+03…
6	152097	[3.4617e+03…
7	6021	[3.3299e+03…
8	5094	[3.3519e+03…
9	24936	[3.5517e+03…
10	9572	[4.0125e+03…
11	6253	[4.1549e+03…
12	32716	[4.5377e+03…
13	13575	[5.0153e+03…

Figure 22 reflects the result of one of the captured images of the concrete plate 06, the post review by the artificial vision system evaluated by the algorithm 03 image and no data values corresponding to specific areas.

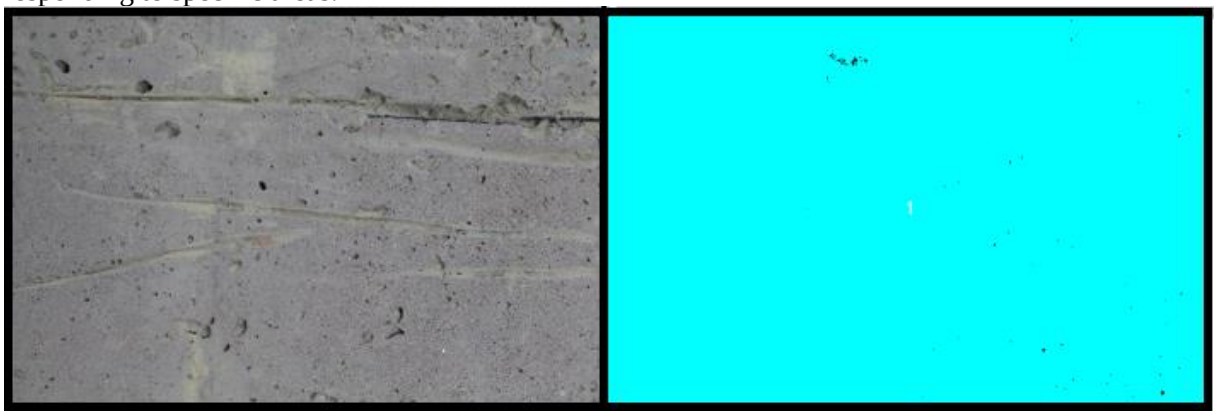

Figure 22 Treatment plate 6 prototype Algorithm 3

Finally, the results of image processing delivered by the algorithm 04 begins in Figure 23, which shows the result of one of the images initially captured from the concrete plate 01 and the image after the revision by the system of artificial vision with a numbering by zones evaluated by the algorithm in the image processing.

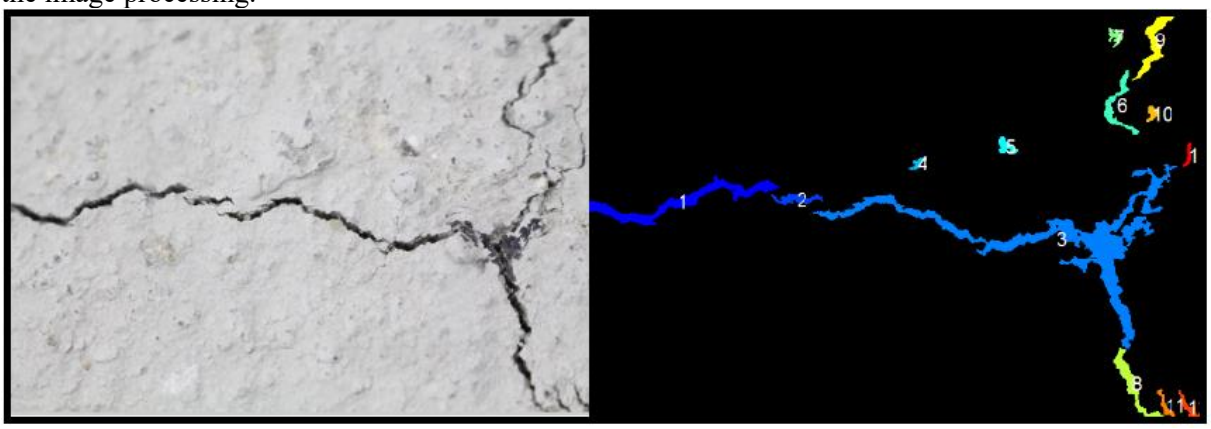

Figure 23 1 Treatment 1 plate prototype Algorithm 4

Table 18 reflects in column 2 the values of the pixel area corresponding to each of the zones evaluated by algorithm 4 on plate 1, Figure 23 shows in the image processed by the algorithm the section corresponding to each number in the first column of the table, additionally in column three is the value of the centroid of the pixelated area by the vision system

Table 18. Data plate processing 1 algorithm 4

Fields	Área	Centroid
1	129900	[783.8090 1…
2	21737	[1.7770e+03…
3	446280	[3.9761e+03…
4	7114	[2.7976e+03…
5	12821	[3.5440e+03…
6	35846	[4.4849e+03…
7	13131	[4.4610e+03…
8	44500	[4.6040e+03…
9	51762	[4.8001e+03…
10	7991	[4.7716e+03…
11	11308	[4.8827e+03…
12	12222	[5.0800e+03…
13	6277	[5.0814e+03…

Figure 24 reflects the result of one of the images initially captured Concrete plate 02 and the image after the revision by the system of artificial vision with a numbering by zones evaluated by the algorithm in the image processing.

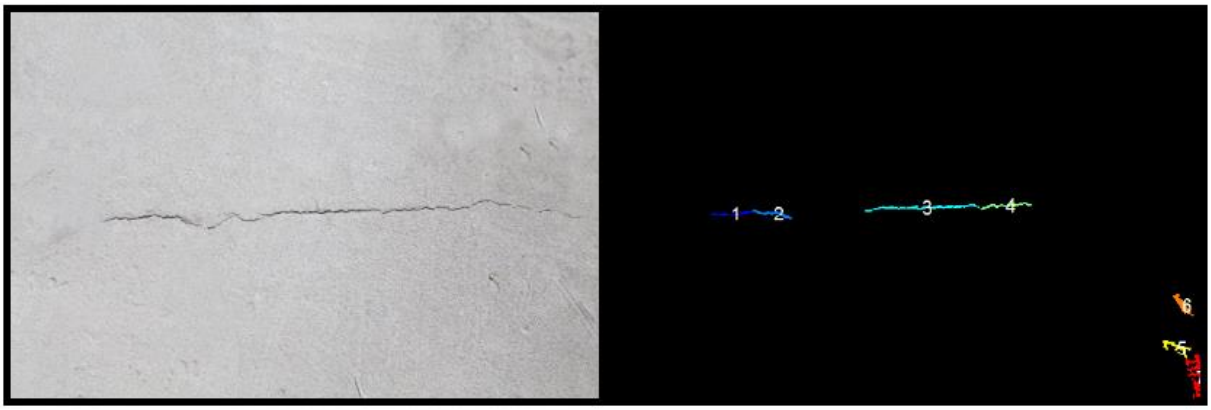

Figure 24 2 Treatment 2 plate prototype Algorithm 4

Table 19 reflects in column 2 the values of the pixel area corresponding to each of the zones evaluated by algorithm 4 on plate 2, Figure 24 shows in the image processed by the algorithm the section corresponding to each number in the first column of the table, additionally in column three is the value of the centroid of the pixelated area by the vision system

Table 19. Data plate processing 2 algorithm 4

Fields	Área	Centroid
1	6848	[1.1394e+03…
2	7986	[1.5189e+03…
3	18582	[2.7841e+03…
4	9008	[3.5020e+03…
5	9707	[4.9660e+03…
6	10743	[5.0147e+03…
7	25924	[5.1364e+03…

Figure 25 reflects the result of one of the images initially captured Concrete plate 03 and the image after the revision by the system of artificial vision with a numbering by zones evaluated by the algorithm in the image processing.

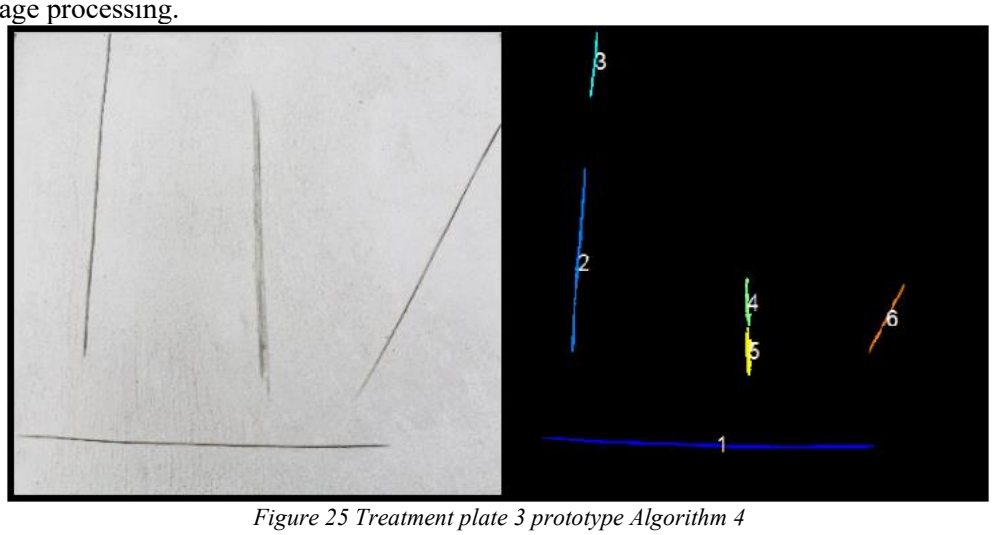

Figure 25 Treatment plate 3 prototype Algorithm 4

Table 20 reflects in column 2 the values of the pixel area corresponding to each of the zones evaluated by algorithm 4 on plate 3, Figure 25 shows in the image processed by the algorithm the section corresponding to each number in the first column of the table, additionally in column three is the value of the centroid of the pixelated area by the vision system

Table 20. Data plate processing 3 algorithm 4

Fields	Área	Centroid
1	45891	[1.5594e+03…
2	23263	[564.2397 1…
3	7686	[680.6746 2…
4	7590	[1.7819e+03…
5	10652	[1.7901e+03…
6	8887	[2.7807e+03…

Figure 26 reflects the result of one of the images initially captured Concrete plate 04 and the image after the revision by the system of artificial vision with a numbering by zones evaluated by the algorithm in the image processing.

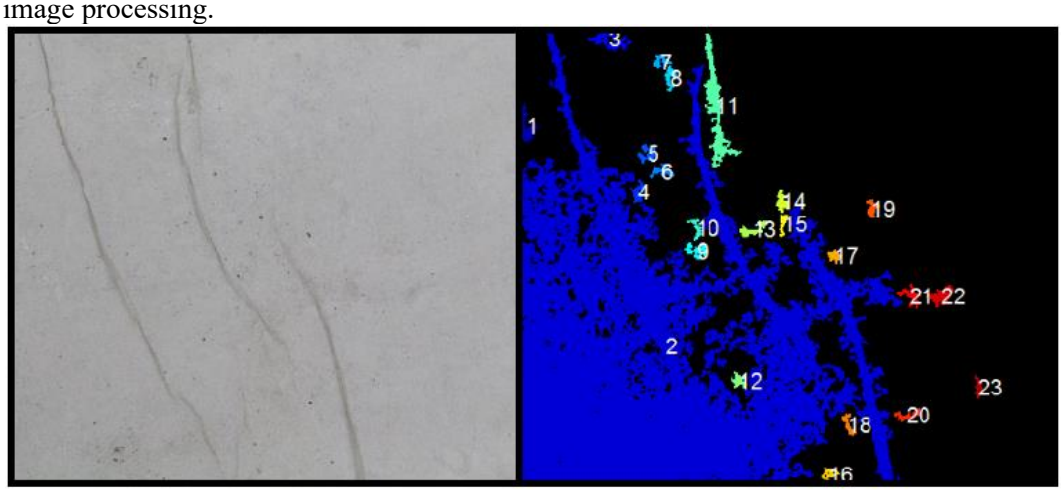

Figure 26 Treatment 4 prototype board Algorithm 4

Table 21 reflects in column 2 the values of the pixel area corresponding to each of the zones evaluated by algorithm 4 on plate 4, Figure 26 shows in the image processed by the algorithm the section corresponding to each number in the first column of the table, additionally in column three is the value of the centroid of the pixelated area by the vision system

Table 21. Data plate processing 4 algorithm 4

Fields	Área	Centroid
1	16997	[40.3358 73…
2	4208663	[1.0683e+03…
3	23418	[650.2943 7…
4	8759	[856.9356 1…
5	10821	[929.6592 9…
6	9499	[1.0350e+03…
7	8269	[1.0276e+03…
8	8214	[1.0960e+03…
9	10150	[1.2868e+03…
10	5782	[1.2802e+03…
11	71969	[1.4260e+03…
12	6842	[1.5909e+03…
13	10382	[1.6994e+03…
14	9071	[1.9133e+03…
15	5510	[1.9195e+03…
16	6172	[2.2605e+03…
17	5801	[2.2949e+03…
18	6868	[2.3935e+03…

19	7730	[2.5705e+03…
20	7943	[2.8252e+03…
21	10750	[2.8450e+03…
22	15664	[3.0767e+03…
23	7051	[3.3490e+03…

Figure 27 reflects the result of one of the images initially captured Concrete plate 05 and the image after the revision by the system of artificial vision with a numbering by zones evaluated by the algorithm in the image processing.

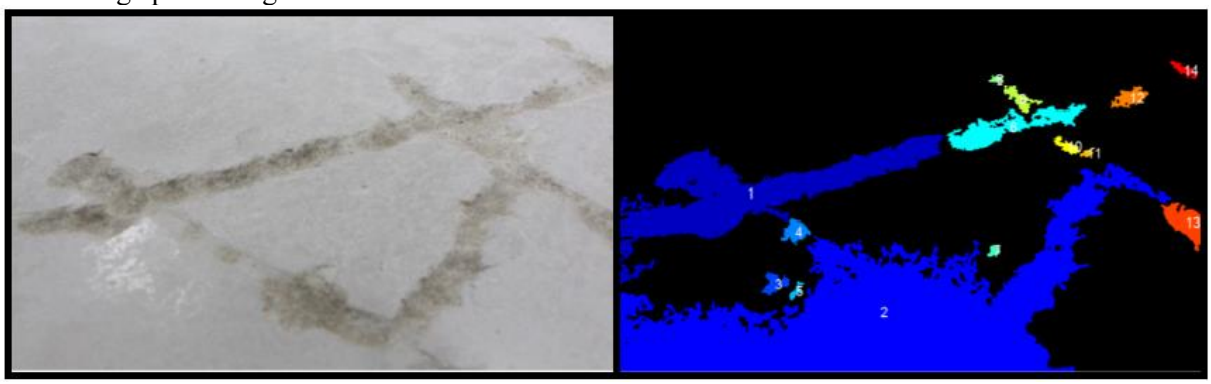

Figure 273 Treatment plate 5 prototype Algorithm 4

Table 22 reflects in column 2 the values of the pixel area corresponding to each of the zones evaluated by algorithm 4 on plate 5, Figure 27 shows in the image processed by the algorithm the section corresponding to each number in the first column of the table, additionally in column three is the value of the centroid of the pixelated area by the vision system.

Table 22. Data plate processing 5 algorithm 4

Fields	Área	Centroid
1	15719	[3.9788e+03…
2	5520	[4.1582e+03…
3	34378	[4.5348e+03…
4	77714	[5.0312e+03…
5	14604	[5.0137e+03…

And Figure 28 reflects the result of one of the images captured from the concrete plate 06, the post-review by the artificial vision system evaluated by the algorithm 04 image and no data values corresponding to the specific areas.

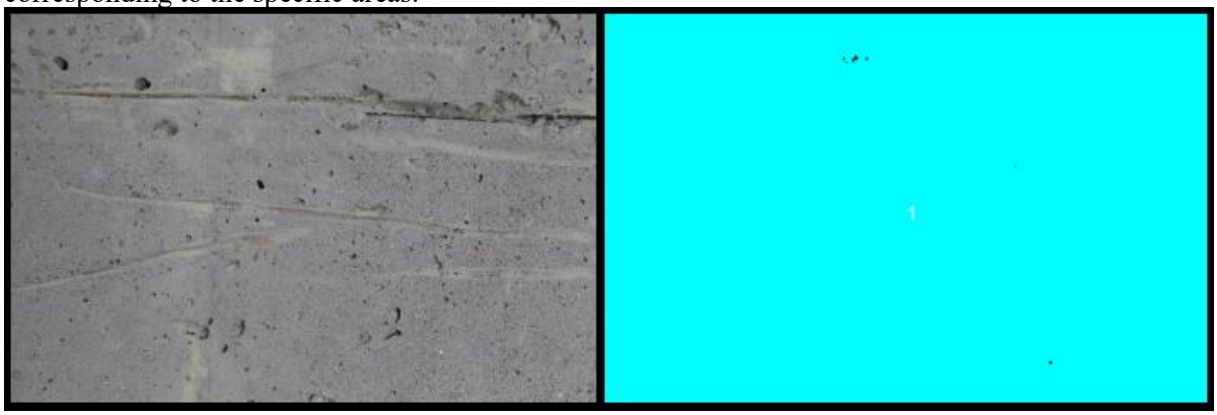

Figure 28 Treatment plate 6 prototype Algorithm 4

Finally, Figure 29 reflects the graphical interface of algorithm management designed for the realization of the crack detection process in flat concrete structures.

Figure 29 Interface artificial vision system

4. Analysis of the results

Image processing is reflected in the figures described in the previous paragraph (Tests and results), have a comparative as Figure 29, in which once the digital imaging procedure in MATLAB performed, the program to analyze the images with tests with the experimental design, identifying cracks and certain additional surface anomalies in the concrete slabs, noting these discontinuities, highlighting the area of the same (square pixels).

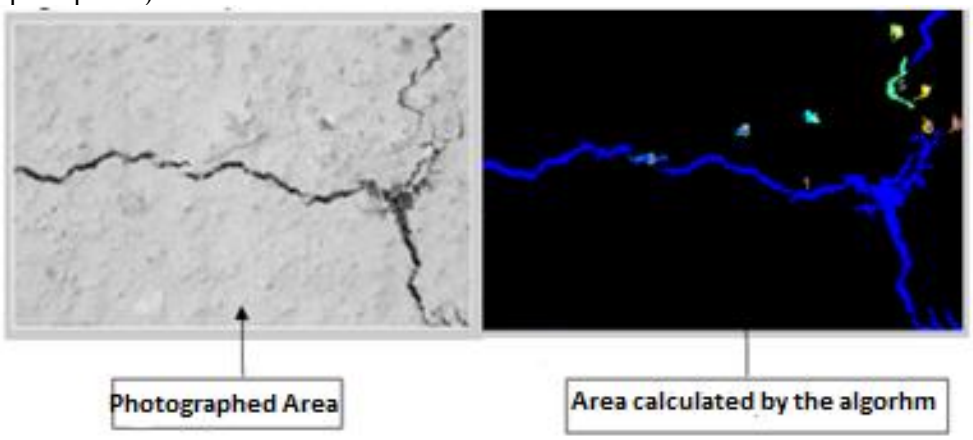

Figure 30 Data treatment

4 prototypes were made, each prototype test on 6 plates to determine which of the four allow detect is cracked plates, in turn determine the impact area thereof. Figures 5, 6,7, 8, 9 and 10 present the results of image processing of the plates 1, 2, 3, 4, 5 and 6 of the algorithm 01 designed, this analysis was replicated with 03 other algorithms. In Figures 5, 6 and 7 corresponding to the first three plates analyzed, images reflect some points marked in the fissures and a shade of blue in the discontinuities, the numbered points above allow calculation by the algorithm the approximate area of the crack. Furthermore, FIG 8 and 9 corresponding to the fourth and fifth plate analyzed, does not generate an image processing so clear, the result is a large percentage of affectation image processing which exceeds the naked eye the affected flat plate in the original photograph area finally figure 10 corresponding to the sixth plate, shows no visible result of cracks despite world. The phenomenon affecting Figures 8, 9 and 10 can occur because the plates have different areas with high concentrations of porosity which would affect the final outcome of digital image processing. shows no visible result of cracks despite world. The phenomenon

affecting Figures 8, 9 and 10 can occur because the plates have different areas with high concentrations of porosity which would affect the final outcome of digital image processing. shows no visible result of cracks despite world. The phenomenon affecting Figures 8, 9 and 10 can occur because the plates have different areas with high concentrations of porosity which would affect the final outcome of digital image processing.

For analysis prototype algorithm 02, the results are reflected in Figures 11, 12, 13, 14, 15 and 16 respectively, for each in ascending order of one sixth plate. Figures 11, 12 and 13 correspond to the analysis in the plates 1, 2 and 3, reflecting an initial taking of the plate, a result of image processing by the algorithm image, and calculating the area of the crack, these results show a fissure type discontinuities visually visible in the initial photograph, but with a level of continuity reflected in the blueness of the result of digital processing inferior to those provided by the algorithm 01. Furthermore image, figure 14 and 15 corresponding to the fourth and fifth plate analyzed, does not generate an image processing so clear, the result is a large percentage of affectation image processing which exceeds the naked eye the affected flat plate in the original photograph area finally figure 16 corresponding to the sixth plate presents no visible result on cracks in spite of the world. The phenomenon affecting Figures 14, 15 and 16 can occur because the plates have different areas in high concentrations of porosity which would affect the final outcome of digital image processing.

The same phenomenon described above with the algorithm 02 applies to the 03, the figure they represent the first three tests with the first 3 plates, reflect a number of discontinuities fissure type visually visible on the original photograph, but with a level of continuity reflected in the blueness of the result of digital processing inferior to those provided by the algorithm 01. Furthermore image, figure 20 and 21 corresponding to the fourth and fifth plate analyzed, does not generate clear images processing and corresponding figure 24 the sixth plate shows no visible result of cracks. In turn, the figures refer to the analysis algorithm 04 is numbered 22, 23, 24, 25, 26 and 27,

Finally, after performing the process of analysis of the results the need to individually compare them arises, considering the algorithm 01 shows a result of scanning the image with a certain degree of accuracy greater naked eye. The plate 3, 4 and 5 did not allow for proper digitization of images due to the different types of discontinuities have cleft type, crack and high levels of porosity.

5. conclusions

The full factorial designs include optimal experiments to study which variables influence the process. In this project, the application only 4 per plate experiments it was determined the location of the main Fissures existing on flat concrete slabs used for the study.

major benefits of full factorial designs are generated when few variables studied are obtained. This is due to the number of experiments grows exponentially with the number of factors. For example, for six factors, the design comprises 64 experiments. These allow estimating 64 results, many of which will be significant. To study a large number of factors, it is more efficient to use only a fraction of a full factorial design. This is highlighted as it was essential for selecting the appropriate algorithm implementing this type of design of experiments and this foundation, helps explain why its use throughout the project.2^6

In each of the tests they were considered two parameters of great importance for identifying cracks as were the threshold and the boundary area, since such discontinuities are texture, size, shape, different color, therefore it performed with different values. This requires a GUIDE where management is facilitated these two variables was performed, generating the identification of the fissure with more continuity. That is, as it increases the threshold increases the chances would find points or objects that do not belong to the crack, so it is important to identify the closest point to the affected zone presenting the fissure, supported by the histogram of each figure.

In turn, when capturing images should take into account external factors since any abnormality present at the time of registration may impact upon scanning the image through artificial vision system,

it is recommended to reduce the minimum noise, excess or lack of light, among others. Significantly, the texture and finish of the concrete (brightness) can influence when taking photos.

Finally, the area of the crack in flat slabs, comprising software (algorithm), performing four prototypes algorithm through an experimental design 24 tests on concrete slabs 6 present in the laboratory automation analyzed. Given the characteristics of the algorithm the results were satisfactory at the time of identifying areas with type discontinuities fissure present, generating a difference between the algorithms considered for the design of factorial experiments yielding as result the algorithm 01 4 analyzed, it generates a digital treatment better than other images,

References

[1] J. Toriac Corral, «Construction pathology, cracks and complications in hormigon works, origin and prevention,» *Ciencia y Sociedad,* vol. 29, nº 1, pp. 72-114, Marzo 2004.

[2] F. Muñoz Salinas y C. J. Mendoza Escobedo, «Durability in reinforced concrete structures from the perspective of the spanish standard force concrete structures» *Concreo y cemento. Investigacion y desarrollo,* vol. 4, nº 1, 2013.

[3] A. Mohan y S. Poobal, «Crack detection using image processing: A critical reniew and analysis,» *Alexandria Engineering Journal,* vol. 57, nº 2, pp. 787-798, 2017.

[4] J. Aboudi, «Stiffness reduction of cracked solids,» *Engineering Fracture Mechanics,* vol. 26, nº 5, pp. 637-650, 1987.

[5] B. Budiansky y R. J. O'connell, «Elastic moduli of a cracked solid,» *International Journal of Solids and Structures,* vol. 12, nº 2, pp. 81-97, 1976.

[6] H. Kim, E. Ahn, S. Cho, M. Shin y S.-H. Sim, «Comparative analysis of image binarization methods for crack identification in concrete structures,» *Cement and Concrete Research,* vol. 99, pp. 53-61, 2017.

[7] D. Dhital y J. Lee, «A Fully Non-Contact Ultrasonic Propagation Imaging System for Closed Surface Crack Evaluation,» *Experimental Mechanics,* vol. 52, nº 8, pp. 1111-1122, 2012.

[8] Y. Fujita y Y. Hamamoto, «A robust automatic crack detection method from noisy concrete surfaces,» *Machine Vision and Applications,* vol. 22, nº 2, pp. 245-254, Marzo 2011.

[9] Y. Qi, B. Wang, S. Li, X. Ren, J. Zhou, Y. Li y J. Mo, «Improved quantitative analysis method for evaluating fatigue cracks in thermal fatigue testing,» *Materials Letters,* vol. 242, pp. 115-118, 2019.

[10] G. Meneghetti, M. Ricotta y G. Pitarresi, «Infrared thermography-based evaluation of the elastic-plastic J-integral to correlate fatigue crack growth data of a stainless steel,» *International Journal of Fatigue,* vol. 125, pp. 149-160, 2019.

[11] N. Pal Kaur, J. K. Shah, S. Majhi y A. Mukherjee, «Healing and simultaneous ultrasonic monitoring of cracks in concrete,» *Materials Today Communications,* vol. 18, pp. 87-99, 2018.

[12] M. Pavana, D. Furfari, B. Ahmad, M. Gharghouri y M. Fitzpatrick, «Fatigue crack growth in a laser shock peened residual stress field,» *International Journal of Fatigue,* vol. 123, pp. 157-167, 2019.

[13] A. de Pannemaecker, J. Buffiere, S. Fouvry y O. Gratona, «In situ fretting fatigue crack propagation analysis using synchrotron X-ray radiography,» *International Journal of Fatigue,* vol. 97, pp. 56-69, 2017.

[14] M. R., A. S, Mohana y Y. Chitkara, *Inspection, Identification and Repair Monitoring of Cracked Concrete structure –An application of Image processing,* IEEE, 2018.

[15] P. Wang y H. Huang, *Comparison analysis on present image-based crack detection methods in concrete structures,* Yantai: IEEE, 2010.

[16] Y. Wang, J. Y. Zhang, J. Xin Liu, Y. Zhanga, Z. P. Chen, C. Guang Li, K. He y R. B. Yan, «Research on Crack Detection Algorithm of the Concrete Bridge Based on Image Processing,» *Procedia Computer Scienc,* vol. 154, pp. 610-616, 2019.

[17] E. Fesslera, E. Andrieu, V. Bonnand, V. Chiaruttini & S. Pierreta, «Relation between crack growth behaviour and crack front morphology under hold-time conditions in DA Inconel 718,» *International Journal of Fatigue,* vol. 96, pp. 17-27, 2017.

[18] P. Wang y H. Huan, *Comparison analysis on present image-based crack detection methods in concrete structures,* IEEE, 2010.

[19] h. Kim, S. Cho, M. Shin y e. Ahn, «Comparative analysis of image binarization methods for crack identification in concrete structures,» *Cement and Concrete Research ,* 2017.

[20] C. Perez, MATLAB and its applications in science and engineering, pearson, Ed., PRENTICE HALL, 2002.

[21] B. Tarazona, J. Marin y M. Diego, *Desing and construction of a vibration analyzer for the detection of cracks and fissures in concrete structures,* Bucaramanga, 2015.

[22] P. D. Medina Varela y A. M. Lopez Reyes, «Critical analysis of the 2k factorial desing on applied cases» *Scientia Et Technica,* vol. XVIII, nº 47, pp. 101-106, Abril 2011.

[23] R. Hernandez Sampieri, C. Collado y P. Baptista, Investigation methodology, Sexta ed., McGRAW-HILL, 2014.